nature geoscience

ARTICLES

PUBLISHED ONLINE: 13 JULY 2009 | DOI: 10.1038/NGEO577

Floral changes across the Triassic/Jurassic boundary linked to flood basalt volcanism

B. van de Schootbrugge[1]*, T. M. Quan[2], S. Lindström[3,4], W. Püttmann[1], C. Heunisch[5], J. Pross[1], J. Fiebig[1], R. Petschick[1], H.-G. Röhling[5], S. Richoz[1], Y. Rosenthal[2] and P. G. Falkowski[2]

One of the five largest mass extinctions of the past 600 million years occurred at the boundary of the Triassic and Jurassic periods, 201.6 million years ago. The loss of marine biodiversity at the time has been linked to extreme greenhouse warming, triggered by the release of carbon dioxide from flood basalt volcanism in the central Atlantic Ocean. In contrast, the biotic turnover in terrestrial ecosystems is not well understood, and cannot be readily reconciled with the effects of massive volcanism. Here we present pollen, spore and geochemical analyses across the Triassic/Jurassic boundary from three drill cores from Germany and Sweden. We show that gymnosperm forests in northwest Europe were transiently replaced by fern and fern-associated vegetation, a pioneer assemblage commonly found in disturbed ecosystems. The Triassic/Jurassic boundary is also marked by an enrichment of polycyclic aromatic hydrocarbons, which, in the absence of charcoal peaks, we interpret as an indication of incomplete combustion of organic matter by ascending flood basalt lava. We conclude that the terrestrial vegetation shift is so severe and wide ranging that it is unlikely to have been triggered by greenhouse warming alone. Instead, we suggest that the release of pollutants such as sulphur dioxide and toxic compounds such as the polycyclic aromatic hydrocarbons may have contributed to the extinction.

The Triassic/Jurassic (T/J) mass-extinction event, one of the 'big five' extinctions in Earth history[1], has increasingly been linked to the eruption of the Central Atlantic Magmatic Province (CAMP), a large igneous province emplaced during the initial rifting of Pangea[2–4]. The sheer volume of erupted basalts (2.3×10^6 km^3) and brevity of emplacement (500–1,500 kyr) centred around the T/J boundary make the eruption of CAMP basalts the key event of the T/J boundary interval[5,6]. The release of more than 8,000 Gt of CO_2 (ref. 7) is thought to have triggered global warming, shallow marine anoxia leading to blooms of prasinophyte green algae[8,9] and carbon cycle perturbations recorded in the stable isotope composition of carbonates and organic matter[2,10–12]. Whereas CAMP volcanism adequately explains biotic change in the marine realm, the link between volcanism and terrestrial floral changes across the T/J boundary remains equivocal[4]. Some early work on pollen and spore assemblages from northwest Europe detected no significant floral changes across the T/J boundary[13], but analyses of macrofloral remains in Greenland show a species-level turnover of 95% (refs 3, 14). Indeed, many plant families survived the extinction event, but newly evolved groups, such as the Bennettitales, clearly suffered setbacks during the Jurassic[4]. Furthermore, the ecologically significant seed fern *Dicroidium* and all peltasperm seed ferns disappeared at the T/J boundary[4]. It remains largely unclear whether elevated pCO_2 alone would be sufficient to drive the transient setback of Late Triassic gymnosperm forests.

Here, we examine three drill cores from southern Germany (Mingolsheim), northern Germany (Mariental) and southern Sweden (Höllviken-2), which span the critical Late Triassic (Rhaetian) to Early Jurassic (Hettangian–Sinemurian) interval for microfloral (palynology) and organic geochemical signs of terrestrial ecosystem collapse. All cores represent coastal to shallow marine settings bordering three separate depositional basins along a ~1,000 km north-to-south transect (Fig. 1). Strong facies changes due to the shallow marine nature of the studied cores make it difficult to exactly pinpoint the position of the T/J boundary in Germany and Sweden. However, we use the last and first occurrences of palynomorphs to characterize a narrow interval in all three cores that encompasses the T/J boundary (see Supplementary Fig. S1). (1) In all three cores the last occurrences (LO) of the typical Late Triassic palynomorphs *Rhaetipollis germanicus* (pollen) and *Rhaetogonyaulax rhaetica* (dinoflagellate cyst) mark the lower part of this interval. (2) The first occurrence (FO) of the pollen *Cerebropollenites thiergartii* marks the upper limit of this boundary interval. (3) In the Mingolsheim core *C. thiergartii* has not been found, but there the first common occurrence (FCO) of *Kraeuselisporites reissingerii* (spore) coincides with the first appearance of the Early Hettangian ammonite *Caloceras johnstoni* (upper part of the lowermost Hettangian *Psiloceras planorbis* Zone). Correlation of Mingolsheim with the proposed global boundary stratotype section of Kuhjoch in Austria[15] shows that the lower part of the Planorbis Zone in Mingolsheim is condensed in the Psilonoten Limestone. In Austria, the first occurrence of the ammonite *Psiloceras spelae* is now taken to mark the T/J boundary[15]. Because in Austria the FO of *P. spelae* coincides with the FCO of *K. reissingerii*, the T/J boundary in Mingolsheim occurs within or at the top of the Psilonoten Limestone. The biostratigraphic correlation also shows that the Triletes Beds are time equivalent with other T/J boundary beds, such as the Schattwald Beds in Austria[16] and the 'Argiles de Levallois' in northern France and

[1]Institute of Geosciences, Goethe University Frankfurt, Altenhöferallee 1, D-60438 Frankfurt am Main, Germany, [2]Institute of Marine and Coastal Sciences, Rutgers, the State University of New Jersey, 71 Dudley Road, New Brunswick, New Jersey 08901, USA, [3]GeoBiosphere Science Centre, Department of Geology, Lund University, Sölvegatan 12, SE-223 62 Lund, Sweden, [4]Geological Survey of Denmark and Greenland, Øster Voldgade 10, DK-1350 Copenhagen, Denmark, [5]State Authority for Mining, Energy and Geology, Stilleweg 2, D-30655 Hannover, Germany.
*e-mail: van.de.Schootbrugge@em.uni-frankfurt.de.

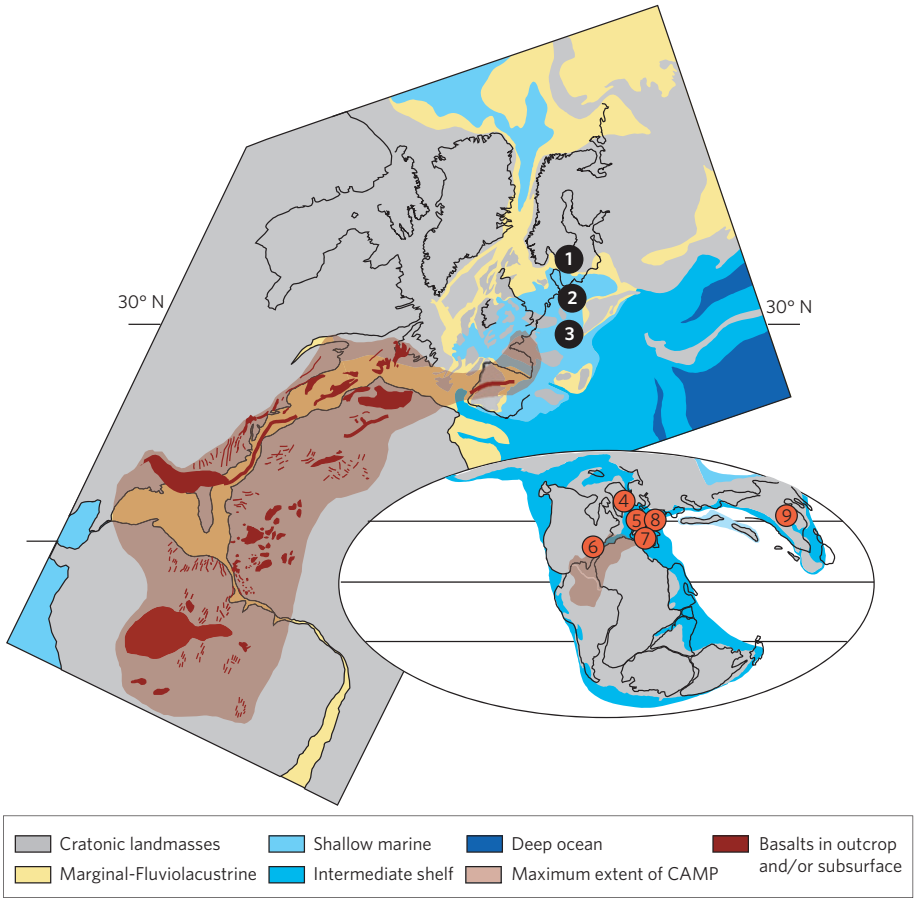

Figure 1 | Distribution of CAMP basalts and T/J boundary fern proliferation. Late Triassic palaeogeographic map showing maximum extent of CAMP basalts and known occurrences of basalt in outcrop and/or subsurface (modified after ref. 44 and Scotese Paleomap Project). Investigated cores: 1 = Höllviken; 2 = Mariental; 3 = Mingolsheim. Other T/J boundary occurrences of fern proliferation: 4 = Greenland[3], 5 = northern France[23], 6 = northeastern US[19], 7 = southern Spain[24], 8 = Austria[16], 9 = northwestern China[20].

Luxemburg[17]. Just as in neighbouring Austria and Luxemburg, the Triletes Beds are a peculiar unbioturbated, extremely carbonate-poor unit that is nearly devoid of marine macrofossils, but rich in trilete lycopod megaspores. The presence of the dinoflagellate cysts *Rhaetogonyaulax rhaetica* and *Dapcodinium priscum* testifies to the shallow marine nature of the Triletes Beds in all three cores.

Floral changes across the Triassic/Jurassic boundary

Our quantitative palynological analyses from the Mingolsheim, Mariental and Höllviken-2 cores (Fig. 2; Supplementary Figs S2 and S3) reveal a remarkably consistent pattern of pertinent floral changes across the Triletes Beds. These vegetation changes start at the base of the Triletes Beds, where typical Rhaetian pollen, such as *Ricciisporites tuberculatus* and *Rhaetipollis germanicus*, decrease significantly in abundance or in the latter case disappear completely (Fig. 2). Moreover, the Triletes Beds mark the transient decline of a latest Triassic arborescent gymnosperm flora dominated by Pinales (predominantly *Corollina* spp.) and cycads–ginkgophytes (for example *Ovalipollis ovalis*, *Monosulcites* spp.). In all cores, this arborescent vegetation is replaced by a latest Rhaetian flora predominantly composed of ground ferns and fern allies (horsetails, tree ferns and mosses). Spores of the Schizaeaceae–Polypodiaceae (*Polypodiisporites polymicroforatus*; Fig. 3), Dipteridaceae–Matoniaceae (for example *Concavisporites* spp.), Osmundaceae (for example *Osmundacidites* spp.) and Equisetaceae (*Calamospora* spp.) make up the bulk of the palynological assemblages. Following the Triletes Beds, Hettangian assemblages are dominated by pollen from Cheirolepidiaceae and Taxodiaceae conifers (for example *Corollina* spp., *Perinopollenites elatoides*, *Pinuspollenites minimus*) and bisaccate pollen from corystosperm seed ferns (for example *Alisporites* spp.). The recovery of conifers is accompanied by a lowermost Hettangian acme of lycopodiophyte spores belonging to the Selaginellales–Isoetales (for example *Kraeuselisporites reissingerii*). Whereas in Mariental and Höllviken-2 fern and tree fern spores (*Concavisporites* spp., *Deltoidospora* spp.) remain abundant throughout the Hettangian, *Polypodiisporites*, which is so characteristic of the Triletes Beds, does not again attain a similar dominance in any of the investigated cores.

Fern proliferation and flood basalt volcanism

Coeval floral changes in northern and southern Germany, and Sweden, are unlikely to have been just the result of a major sea-level fall promoting riparian growth on exposed shelves, followed by rapid Early Jurassic transgression. First, there were multiple, equally large sea-level pulses during the middle Rhaetian and lower Hettangian[18] that did not trigger the same dramatic response of conifer retreat and fern proliferation. Second, T/J boundary fern spikes have also been documented in continental successions in the Newark Basin (northeastern US; ref. 19), Greenland[4] and the Junggar Basin (China; ref. 20). Whereas there is increasing doubt that the fern spike in the Newark Basin really marks the T/J boundary[21], ferns do proliferate directly before deposition of the Orange Mountain Basalt[19]. Third, Schizaeaceae–Polypodiaceae fern spores (also sometimes identified as *Convolutispora microrugulata*) and Dipteridaceae fern spores dominate T/J boundary assemblages in Hungary[22], Austria[16], Luxemburg[17], France[23] and even northern

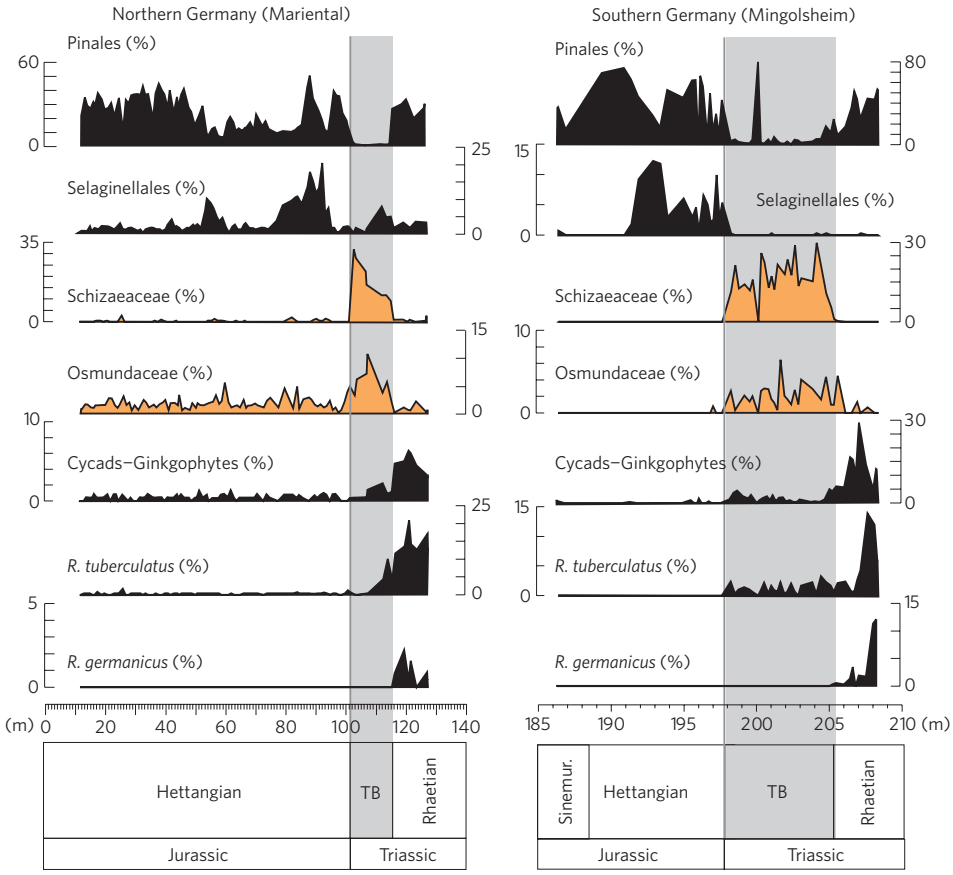

Figure 2 | Floral changes across the T/J boundary as reconstructed from pollen and spores. All pollen and spore data from Mingolsheim and Mariental are presented as percentages of total palynomorph fraction, which also includes marine palynomorphs (dinoflagellate cysts, acritarchs, prasinophytes). Both pollen diagrams show gradual, but pertinent, floral changes across the T/J boundary with the disappearance of typical Late Triassic tree pollen and its transient replacement by spores of ferns and fern allies. Pollen and spores included in the illustrated floral groups: Pinales—*Corollina*, *Pinuspollenites*, *Granuperculatipollis*, *Perinopollenites*, *Cerebropollenites*. Selaginellales–Isoetales—*Kraeuselisporites*, *Uvaesporites*, *Lundbladispora*. Schizaeaceae—*Polypodiisporites*. Osmundaceae—*Punctatisporites*, *Osmundacidites*, *Baculatisporites*. Cycads–Ginkgophytes—*Ovalipollis*, *Monosulcites*, *Chasmatosporites*, *Cycadopites*. TB: Triletes Beds.

Spain[24]. This peculiar fern vegetation thus extended across more than 2,000 km. In contrast, in the Southern Hemisphere, for example in New Zealand, a restructuring of Gondwanan *Dicroidium* floras towards a vegetation composed of cheirolepid conifers progressed without the transient development of a fern-dominated flora[25].

The overwhelming dominance of pteridophytes within the T/J boundary interval is readily explained by their tolerance of stressful habitats, including strongly leached, nutrient-poor or metal-enriched soils, their ability to photosynthesize under low-light conditions, and certain life-cycle traits such as gametophytic selfing and wind dispersal of spores that aid pioneers to rapidly invade disturbed habitats[26]. Horsetails are abundant within the Triletes Beds in all three cores, and *Equisetites muensteri* is the only plant that is present both before and after the T/J boundary in Greenland[3]. Horsetails are able to reproduce through segmentation of underground rhizomes, allowing them to rapidly colonize disturbed areas, as was observed after the eruption of Mount St Helens[27]. Similarly, Dipteridaceae and Schizaeaceae include many members that are early pioneers of disturbed environments[28]. Notably, Schizaeaceae were the first plants to colonize a barren landscape in the aftermath of a volcanic eruption that gave rise to the famous Eocene fossil lagerstätte in Messel (Germany)[29]. Primary successional vegetation communities associated with the Palaeogene Mull Lava Field (Scotland) have also been shown to be dominated by bryophytes and polypodiaceous ferns[30].

Could climate change, induced by CO_2 released from CAMP flood basalt volcanism, explain a proliferation of ferns and fern allies in T/J boundary beds in the Northern Hemisphere? Ferns require moisture for their reproductive cycles, hence we exclude 'global drying' as an explanation, in agreement with previous studies[3]. Clay mineral analyses document high amounts of kaolinite in the Triletes Beds (Supplementary Figs S2,S3), which is typical of strongly leached soils that become progressively enriched in aluminium. Based on sedimentological and clay mineralogical analyses of Rhaetian palaeosols, it was concluded that the latest Triassic witnessed extremely humid climate conditions across northern Europe[31]. Whereas we do not discount the role of climate changes in the T/J boundary proliferation of pteridophytes, we deem it improbable that a mere increase in precipitation due to greenhouse warming could have triggered rampant growth of only a few fern species over such a vast area.

As well as CO_2, other volcanic pollutants, particularly sulphur dioxide (SO_2), are increasingly thought of as the main agents of environmental change during the emplacement of large igneous provinces[32,33]. The role of SO_2 has generally been ignored, because sulphate aerosols (sulphuric acid droplets (H_2SO_4) formed by the reaction of SO_2 with hydroxyl radicals) are very short lived and are washed out of the atmosphere after days to months. Hence, global cooling and the inhibition of photosynthesis triggered by sulphate aerosol darkening seems problematic as a valid mechanism for the observed floral changes[34]. Two recent case studies, however,

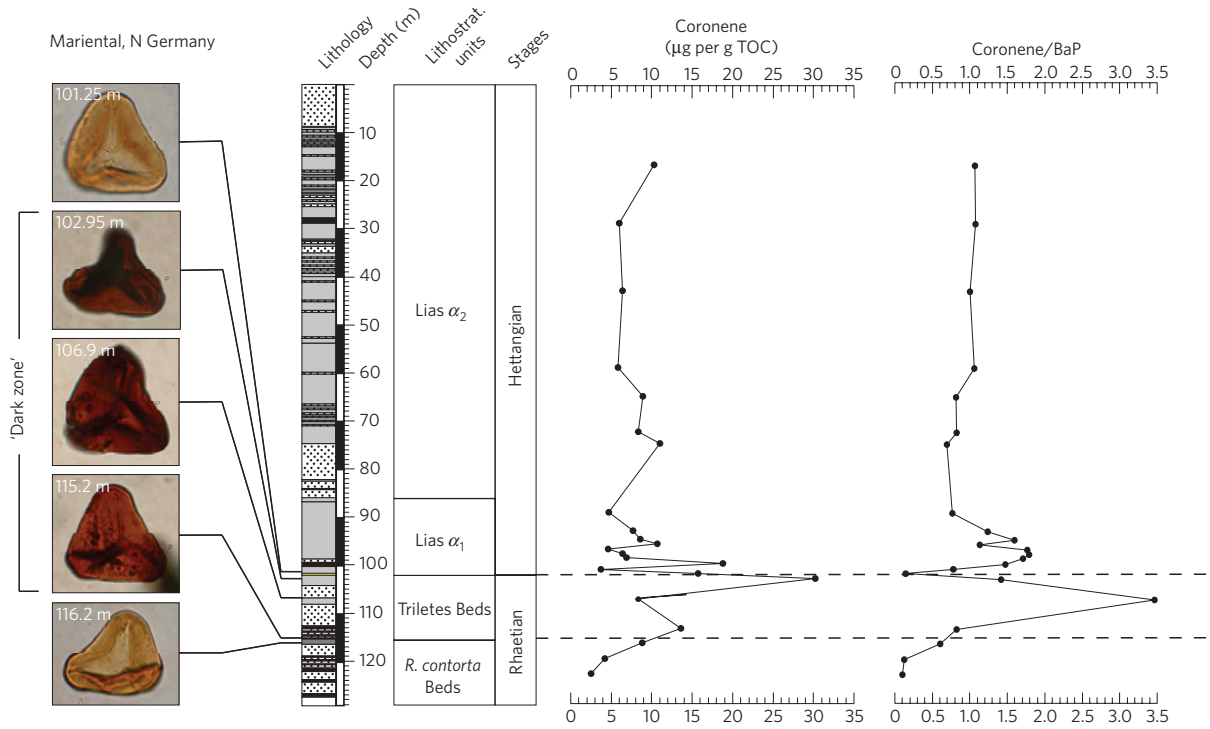

Figure 3 | A T/J boundary 'dark zone'. Palynomorphs in the Triletes Beds show a marked darkening in all three cores, here exemplified by trilete spores of the *Concavisporites–Deltoidospora* complex. This phenomenon occurs throughout the Danish–German basin and beyond. The Triletes Beds also stand out because of elevated quantities of polycyclic aromatic hydrocarbons, such as coronene (shown here in µg per g of total organic carbon, TOC) and benzo(a)pyrene (BaP). The high ratio of coronene relative to benzo(a)pyrene is taken as evidence for a volcanic source of the polycyclic aromatic hydrocarbons.

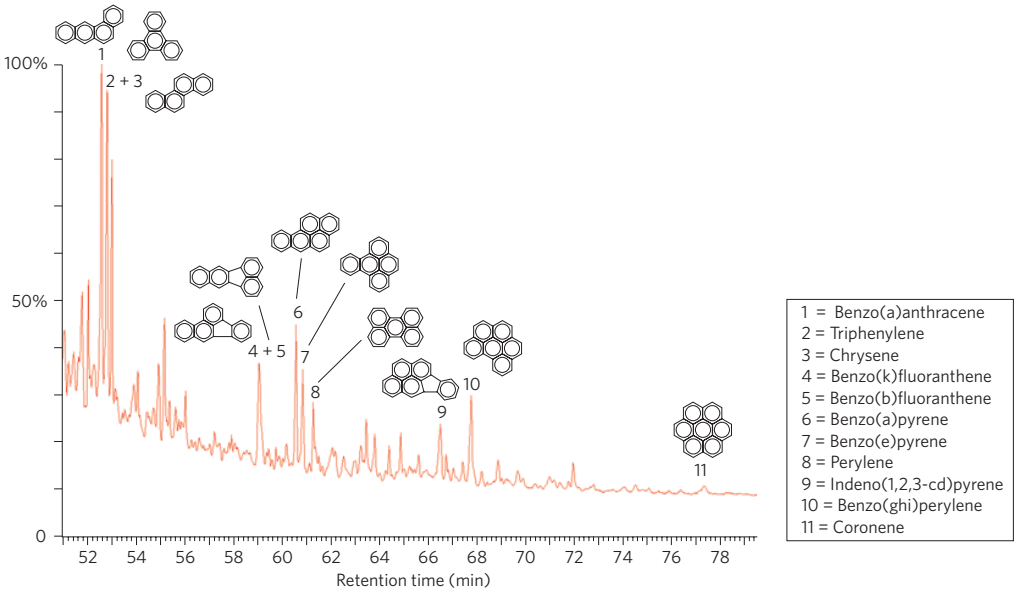

Figure 4 | PAH in T/J boundary beds. Total-ion-current chromatogram of a typical Triletes Bed sample from the Mariental core (sample 101.80 m) and the identified four-, five- and six-ring pyrogenic PAH.

have significantly altered our perception of the devastating effects of subaerial flood basalt eruptions. Improved dating techniques show that the emplacement of the end-Cretaceous Deccan Traps proceeded in several extremely large and rapid pulses[35,36], implying SO_2 emission rates of several Gt yr^{-1} for single eruptive events in the Deccan Traps (that is, 1,000 times above present-day volcanic degassing rates of 9 Mt yr^{-1} as SO_2; ref. 37). Furthermore, work on the end-Permian Siberian Traps suggests that the exhalation of pollutants, such as CO_2, CH_4, halocarbons and SO_2, may have been exacerbated by the heating of Palaeozoic petroleum source rocks and evaporites that were intruded by ascending lava[38].

Organic geochemical evidence for CAMP activity

Organic geochemical analyses of the Triletes Beds from the Mariental core provide direct evidence for a scenario in which organic rich sediments intruded by CAMP basalts take centre stage.

Coinciding with fern proliferation we find elevated amounts of polycyclic aromatic hydrocarbons (PAH; Fig. 3). PAH dominate in the upper boiling point range of the gas chromatograms of total extracts of samples originating from the Triletes Beds (Fig. 4). The dominant PAH are the high-molecular-weight four-ring aromatics, notably benzo(a)anthracene (1), triphenylene (2) and chrysene (3), and the five-ring aromatics benzo(k)fluoranthene (4), benzo(b)fluoranthene (5), benzo(a)pyrene (6), benzo(e)pyrene (7) and perylene (8). Among the heavier PAHs (>5-ring) identified, indeno[1,2,3-cd]pyrene (9), benzo(ghi)perylene (10) and coronene (11) are the most abundant (Fig. 4). PAH can have various origins ranging from petrogenic (diagenesis of sedimentary organic matter) to pyrogenic (combustion of organic matter), but the high intensities of benzo(a)pyrene, benzo(ghi)perylene and coronene suggest that the PAH in the Triletes Beds are pyrolytic products that stem either from forest fires or from volcanic activity. A suite of PAH similar to those found here has been identified in tephra in Iceland[39]. Palynofacies analyses of Mariental samples do not show strong variations in black opaque phytoclasts[40] that could point to increased levels of charcoal, and which correlate with the PAH abundance. However, further work is warranted, because it is difficult to distinguish charcoal from other black phytoclasts without vitrinite reflectance analyses. Still, we deem intensified forest-fire activity during the latest Rhaetian unlikely owing to extremely humid climate conditions, which can be inferred from clay mineral analyses. Ratios of various PAH have been used to constrain their origins. In particular, high coronene to benzo(a)pyrene ratios (Fig. 3) suggest that the PAH in Mariental do reflect other sources than forest fires[41]. We thus interpret elevated amounts of PAHs within the Triletes Beds in Mariental to derive mainly from volcanic activity, presumably through incomplete subsurface burning of coal beds under high temperature and in the absence of free oxygen. Late Triassic Carnian coal deposits and evaporites in the Newark rift[42,43], and Permian evaporites in Brazil[38] are known to have been intruded by CAMP basalts, releasing possibly well in excess of the 8,000 Gt of CO_2 and 2,300 Gt of SO_2 that follow from model calculations[7,44].

Once released into the environment, PAH easily adsorb onto atmospheric particles, such as sulphate aerosols, which transported PAH from CAMP basalts to NW Europe. Polycyclic aromatic hydrocarbons are extremely toxic and benzo(a)pyrene is known to be strongly carcinogenic[41]. It has been postulated[38] that the release of large quantities of brominated and chlorinated halocarbons from heated evaporites may lead to a severe loss of stratospheric ozone, thereby increasing lethal radiation. Based on our low-resolution study it is too early to identify the direct role of PAH release in the T/J mass-extinction event, be it environmental pollution or atmospheric damage. A puzzling feature associated with the Triletes Beds in all three cores is the marked change in colour of pollen and spores. Palynomorphs within the Triletes Beds are much darker than those palynomorphs from the underlying Rhaetian and the overlying Hettangian (Fig. 3). This 'dark zone' is well known among Mesozoic palynologists because it serves as a good stratigraphic indicator for the end-Triassic in Europe[45]. Colour changes have been reported from the Eitzendorf-8 core from northern Germany[46], the Rødby-1 core in Denmark[46] and various cores in Sweden[47]. According to ref. 45, spore colour ranges from a thermal alteration index value of 2.6 below and above the T/J boundary to 3.0 within the boundary interval[45]. Since all three cores experienced different burial histories, the colour change cannot be the result of increased thermal maturity due to overburden. Darkening of palynomorphs can be induced artificially by reacting them with acetic anhydride and sulphuric acid (acetolysis). This is a routine procedure during palynological preparations, and serves to increase the visibility for light microscopy of otherwise sometimes pale and colourless palynomorphs[48]. None of our samples were prepared in this way, hence the colour changes were clearly the result of natural processes. Although speculative, we suggest that the dark colour of palynomorphs within the Triletes Beds may have been caused by soil acidification from sulphuric acid deposition during CAMP eruptions.

Coeval PAH enrichment and proliferation of ferns in T/J boundary beds point to a strong link between flood basalt volcanism and perturbations in terrestrial ecosystems. In our scenario, which may also hold true for other mass-extinction events associated with subaerial flood basalts, CO_2, SO_2 and other pollutants exerted direct environmental stress on terrestrial floras through greenhouse warming, soil acidification and possibly atmospheric damage.

Methods

Palynology. For palynology, 8–10 g of bulk rock was treated in alternating steps with hydrochloric (38%) and hydrofluoric acid (40%) to remove carbonate and silicate mineral phases. After washing to neutrality, residues were sieved with 15 μm mesh-size sieves to remove clay minerals and palynomorphs were mounted on strew slides. 300 palynomorphs were counted per sample from Mingolsheim (56 samples), except for a few Hettangian samples, where pollen sums of 100 were reached owing to large amounts of amorphous organic matter. From each sample from Mariental 200 palynomorphs were counted (98 samples). From Höllviken-2 also 300 palynomorphs were counted per sample (17 samples). Counting proceeded with compound microscopes at ×400–630 magnification. Data were calculated as percentages of the total palynomorph assemblage.

Clay mineral analyses. Clay mineral analyses were performed on carefully ground fine-grained material separated by the use of Stokes's law (<2 μm equivalent diameter). Samples were evaporated and aliquots with uniform amount of 4 mg cm^{-2} were analysed using a Philips X-ray diffractometer at the Institute of Geosciences of Frankfurt University, equipped with a Cu fine focus tube (40 kV, 30 mA), automated divergence slit and secondary monochromator. Peak-area ratios of detected main clay minerals were determined by the use of *MacDiff* software. Expandable clay minerals, such as smectite, were detected after standard ethylene glycol treatment.

Organic geochemistry. For total organic carbon content measurements the samples were pretreated with concentrated hydrochloric acid to remove carbonates. Organic carbon contents (wt%) were measured using a EURO Elemental Analyser from Eurovectors Instruments. Approximately 2 mg of each sample was combusted in an oxygen stream at a temperature of 1,350 °C. The generated CO_2 was separated by gas chromatography from the combustion gas and then quantified using a thermal conductivity detector. For Soxhlet extraction 15 g of each sediment sample were finely ground (<0.2 mm) and extracted for 24 h in a Soxhlet extraction apparatus using 200 ml dichloromethane as solvent. The total extracts were analysed by gas chromatography–mass spectrometry. Gas chromatography–mass spectrometry analyses were carried out on a TraceUltra GC (ThermoFisher Scientific) coupled to a Trace DSQ II (ThermoFisher Scientific) mass spectrometer. Separation of the compounds was achieved using a fused silica capillary column (Thermo TR-5 ms SQC, 15 m × 0.25 mm ID × 0.25 μm film thickness). The oven temperature was programmed from 60 to 300 °C at a rate of 4 °C min^{-1}, with a 20 min isothermal period at 300 °C. The samples were injected in the splitless mode with the injector temperature at 280 °C. Helium was used as carrier gas. The mass spectrometer was operated in the electron impact mode at 70 eV ionization energy. Mass spectra were obtained by scanning from 45 to 700 Da at a cycle time of 1 s. For data processing, the Exalibur software (ThermoFisher Scientific) was used. Identification of compounds was made by comparison of mass spectra and on the basis of retention times using standard compounds supplied by Ehrendorfer GmbH. For quantification, 1,1′-binaphthyl was added to the total extracts. The selected PAH were quantified from the related mass chromatograms: mass-to-charge ratio m/z 228 for benzo(a)anthracene, m/z 252 for benzo(a)pyrene, m/z 276 for benzo(ghi)perylene and m/z 300 for coronene. Response factors of these four compounds in relation to 1,1′-binaphthyl were determined from a solution containing all five compounds at a concentration of 1 μg l^{-1}.

Received 17 April 2009; accepted 16 June 2009; published online 13 July 2009

References

1. Raup, D. M. & Sepkoski, J. J. Jr Mass extinctions in the marine fossil record. *Science* **215**, 1501–1503 (1982).
2. Hesselbo, S. P., Robinson, S. A., Surlyk, F. & Piasecki, S. Terrestrial and marine extinction at the Triassic–Jurassic boundary synchronized with major carbon cycle perturbation: A link to initiation of massive volcanism. *Geology* **30**, 251–254 (2002).
3. McElwain, J. C., Beerling, D. J. & Woodward, F. I. Fossil plants and global warming at the Triassic–Jurassic boundary. *Science* **285**, 1386–1390 (1999).

4. McElwain, J. C., Popa, M. E., Hesselbo, S. P., Haworth, M. & Surlyk, F. Macroecological responses of terrestrial vegetation to climatic and atmospheric change across the Triassic/Jurassic boundary in East Greenland. *Paleobiology* **33**, 547–573 (2007).
5. Marzoli, A. *et al.* Extensive 200-million-year-old continental flood basalts of the Central Atlantic Magmatic Province. *Science* **284**, 616–618 (1999).
6. Marzoli, A. *et al.* Synchrony of the Central Magmatic Province and the Triassic–Jurassic boundary and biotic crisis. *Geology* **32**, 973–976 (2004).
7. Beerling, D. J. & Berner, R. A. Biogeochemical constraints on the Triassic–Jurassic boundary carbon cycle event. *Glob. Biogeochem. Cycles* **16**, 10(11)–10(13) (2002).
8. Quan, T. M., van de Schootbrugge, B., Field, P., Rosenthal, Y. & Falkowski, P. G. Nitrogen isotope and trace metal analyses from the Mingolsheim core (Germany): Evidence for redox variations across the Triassic–Jurassic boundary. *Glob. Biogeochem. Cycles* **22**, GB2014 (2008).
9. van de Schootbrugge, B. *et al.* End-Triassic calcification crisis and blooms of organic-walled disaster species. *Palaeogeogr. Palaeoclimatol. Palaeoecol.* **244**, 126–141 (2007).
10. Galli, M. T., Jadoul, F., Bernasconi, S. M. & Weissert, H. Anomalies in global carbon cycling and extinction at the Triassic/Jurassic boundary: Evidence from a marine C-isotope record. *Palaeogeogr. Palaeoclimatol. Palaeoecol.* **216**, 203–214 (2005).
11. Galli, M. T., Jadoul, F., Bernasconi, S. M., Cirilli, S. & Weissert, H. Stratigraphy and palaeoenvironmental analysis of the Triassic–Jurassic transition in the western Southern Alps (Northern Italy). *Palaeogeogr. Palaeoclimatol. Palaeoecol.* **244**, 52–70 (2007).
12. van de Schootbrugge, B. *et al.* Carbon cycle perturbation and stabilization in the wake of the Triassic–Jurassic boundary mass-extinction event. *Geochem. Geophys. Geosyst.* **9**, Q04028 (2008).
13. Fisher, M. J. & Dunay, R. E. Palynology and the Triassic/Jurassic boundary. *Rev. Palaeobot. Palyno.* **34**, 129–135 (1981).
14. Pedersen, K. R. & Lund, J. J. Palynology of the plant-bearing Rhaetian to Hettangian Kap Stewart formation, Scoresby Sund, East Greenland. *Rev. Palaeobot. Palyno.* **281**, 1–69 (1980).
15. Ruhl, M., Kürschner, W. M. & Krystyn, L. Triassic–Jurassic organic carbon isotope stratigraphy of key sections in the western Tethys realm (Austria). *Earth Planet. Sci. Lett.* **281**, 169–187 (2009).
16. Kürschner, W. M., Bonis, N. & Krysytn, L. Carbon isotope stratigraphy and palynostratigraphy of the Triassic–Jurassic transition in the Tiefengraben section—Northern Calcareous Alps (Austria). *Palaeogeogr. Palaeoclimatol. Palaeoecol.* **244**, 257–280 (2007).
17. Schuurman, W. L. Aspects of Late Triassic palynology. 2. Palynology of the Gres et Schiste a Avicula contorta and Argiles de Levallois (Rhaetian) of northeastern France and southern Luxemburg. *Rev. Palaeobot. Palyno.* **23**, 159–253 (1977).
18. De Graciansky, P.-C., Jacquin, T. & Hesselbo, S. P. in *Mesozoic and Cenozoic Sequence Stratigraphy of European Basins* Special Publication 60 (eds De Graciansky, P.-C., Hardenbol, J., Jacquin, T. & Vail, P. R.) (SEPM, 1998).
19. Olsen, P. E. *et al.* Ascent of dinosaurs linked to an iridium anomaly at the Triassic–Jurassic boundary. *Science* **296**, 1305–1307 (2002).
20. Lu, Y. & Deng, S. Triassic–Jurassic sporopollen assemblages on the southern margin of the Junggar Basin, Xinjiang and the T–J boundary. *Acta Geol. Sin.* **79**, 15–28 (2005).
21. Lucas, S. G. & Tanner, L. H. The nonmarine Triassic–Jurassic boundary in the Newark Supergroup of eastern North America. *Earth Sci. Rev.* **84**, 1–20 (2007).
22. Götz, A. E., Ruckwied, K., Palfy, J. & Haas, J. Palynological evidence for synchronous changes within the terrestrial and marine realm at the Triassic–Jurassic boundary (Csövàr section, Hungary). *Rev. Palaeobot. Palyno.* doi: 10.1016/j.revpalbo.2009.04.002 (2009).
23. Rauscher, R., Hilly, J., Hanzo, M. & Marchal, C. Palynologie des couches de passage du Trias superieure au Lias dans l'est du Bassin Parisien. Problemes de datation du 'Rhetien' de Lorraine. *Sci. Geol. Bull.* **48**, 159–185 (1995).
24. Gomez, J. J., Goy, A. & Barron, E. Events around the Triassic–Jurassic boundary in northern and eastern Spain: A review. *Palaeogeogr. Palaeoclimatol. Palaeoecol.* **244**, 89–110 (2007).
25. Zhang, W. & Grant-Mackie, J. A. Late Triassic–Early Jurassic palynofloral assemblages from Murihiku strata of New Zealand and comparisons with China. *J. R. Soc. New Zealand* **31**, 575–683 (2001).
26. Page, C. N. Ecological strategies in fern evolution: A neopteridological overview. *Rev. Palaeobot. Palyno.* **119**, 1–33 (2002).
27. Rothwell, G. W. Pteridophytic evolution: An often underappreciated phytological success story. *Rev. Palaeobot. Palyno.* **90**, 209–222 (1996).
28. Collinson, M. E. The ecology of Cainozoic ferns. *Rev. Palaeobot. Palyno.* **119**, 51–68 (2002).
29. Lenz, O. K., Wilde, V. & Riegel, W. Recolonization of a Middle Eocene volcanic site: Quantitative palynology of the initial phase of the maar lake of Messel (Germany). *Rev. Palaeobot. Palyno.* **145**, 217–242 (2007).
30. Jolley, D. W., Bell, B. R., Williamson, I. T. & Prince, I. Syn-eruption vegetation dynamics, paleosurfaces and structural controls on lava field vegetation: An example from the Palaeogene Staffa Formation, Mull Lava Field, Scotland. *Rev. Palaeobot. Palyno.* **153**, 19–33 (2009).
31. Ahlberg, A., Olsson, I. & Simkevicius, P. Triassic–Jurassic weathering and clay mineral dispersal in basement areas and sedimentary basins of southern Sweden. *Sediment. Geol.* **161**, 15–29 (2003).
32. Self, S., Widdowson, M., Thordarson, T. & Jay, A. E. Volatile fluxes during flood basalt eruptions and potential effects on the global environment: A Deccan perspective. *Earth Planet. Sci. Lett.* **248**, 518–532 (2006).
33. Chenet, A.-L., Fluteau, F. & Courtillot, V. Modelling massive sulphate aerosol pollution, following the large 1783 Laki basaltic eruption. *Earth Planet. Sci. Lett.* **236**, 721–731 (2005).
34. Guex, J., Bartolini, A., Atudorei, V. & Taylor, D. High-resolution ammonite and carbon isotope stratigraphy across the Triassic–Jurassic boundary at New York Canyon (Nevada). *Earth Planet. Sci. Lett.* **225**, 29–41 (2004).
35. Chenet, A.-L., Fluteau, F., Courtillot, V., Gerard, M. & Subbarao, K. V. Determination of rapid Deccan eruptions across the Cretaceous–Tertiary boundary using paleomagnetic secular variation: Results from a 1200-m thick section in the Mahabaleshwar escarpment. *J. Geophys. Res.* **113**, B04101 (2008).
36. Chenet, A.-L., Quidelleur, X., Fluteau, F., Courtillot, V. & Bajpai, S. 40 K-40Ar dating of the Main Deccan large igneous province: Further evidence of KTB age and short duration. *Earth Planet. Sci. Lett.* **263**, 1–15 (2007).
37. Halmer, M. M., Schmincke, H.-U. & Graf, H.-F. The annual volcanic gas input into the atmosphere, in particular into the stratosphere: A global data set for the past 100 years. *J. Volcanol. Geothermal Res.* **115**, 511–528 (2002).
38. Svensen, H. *et al.* Siberian gas venting and the end-Permian environmental crisis. *Earth Planet. Sci. Lett.* **277**, 490–500 (2009).
39. Geptner, A. R., Alekseeva, T. A. & Pikovskii, Y. I. Polycyclic aromatic hydrocarbons in Holocene sediments and tephra of Iceland (composition and distribution features). *Lithol. Mineral Resour.* **37**, 148–156 (2002).
40. Heunisch, C., Luppold, F. W., Reinhardt, L. & Röhling, H.-G. Palynofazies, Bio-, und Lithostratigraphie im Grenzbereich Rhät/Lias in der Bohrung Mariental I (Lappwaldmulde, Ostniedersachsen). *Zeitschrift der Deutschen Geologischen Gesellschaft* (in the press).
41. Freeman, D. J. & Cattell, F. C. R. Woodburning as a source of atmospheric polycyclic aromatic hydrocarbons. *Environ. Sci. Technol.* **24**, 1581–1585 (1990).
42. Robbins, E. I., Wilkes, G. P. & Textoris, D. A. in *Triassic–Jurassic Rifting: Continental Break-up and the Origin of the Atlantic Ocean and Passive Margins* (ed. Manspeizer, W.) 649–682 (Part B, Developments in Geotectonics, Elsevier, 1988).
43. van Houten, F. B. Contact metamorphic mineral assemblages, Late Triassic Newark Group, New Jersey. *Contrib. Mineral. Petrol.* **30**, 1–14 (1971).
44. McHone, J. G. *The Central Atlantic Magmatic Province* 1–13 (American Geophysical Union, 2002).
45. Lund, J. J. Rhaetian to Pliensbachian palynostratigraphy of the central part of the NW German Basin exemplified by the Eitzendorf 8 well. *Cour. Forsch. Inst. Senckenberg* **241**, 69–83 (2003).
46. Lund, J. J. Rhaetic to lower Jurassic palynology of the onshore southeastern North Sea Basin. *Danmarks Geologiske Undersogelse II Raekke* **109**, 1–129 (1977).
47. Lindström, S. & Erlström, M. The late Rhaetian transgression in southern Sweden: Regional (and global) recognition and relation to the Triassic–Jurassic boundary. *Palaeogeogr. Palaeoclimatol. Palaeoecol.* **241**, 339–372 (2006).
48. Traverse, A. *Paleopalynology* (Unwin Hyman, 1988).

Acknowledgements

We thank C. Christ (Frankfurt University) for her help with the quantification of the PAH and E. Gottwald (Frankfurt University) for continued support in terms of rock preparation. Discussions with H. Visscher (Utrecht University), J. Payne (Stanford University), H. Jenkyns and S. Hesselbo (Oxford University) helped to shape ideas presented here. J. van Konijnenburg-van Cittert (Utrecht University) is warmly thanked for her advice on palaeobotanical affinities of identified palynomorphs. B.v.d.S. acknowledges financial support from the German Science Foundation (DFG) project Scho-1216/2. S.L. acknowledges financial support from the Swedish Geological Survey (SGU) and the Crafoord Foundation.

Author contributions

B.v.d.S., S.L. and C.H. were responsible for generating the palynological data from Mingolsheim, Höllviken-2 and Mariental, respectively, and were involved in writing. W.P. analysed samples from Mariental for biomarkers and assisted with the interpretation. H.-G.R. was responsible for drilling the Mariental core and provided important lithologic and stratigraphic information. R.P. generated the clay mineral data and helped with the discussion. J.P. and S.R. contributed on the palaeoecological and biostratigraphic interpretations. J.F., T.M.Q., Y.R. and P.G.F. contributed to the text.

Additional information

Supplementary information accompanies this paper on www.nature.com/naturegeoscience. Reprints and permissions information is available online at http://npg.nature.com/reprintsandpermissions. Correspondence and requests for materials should be addressed to B.v.d.S.